ACADEMIA ROMÂNĂ
Revue Roumaine de Chimie
http://web.icf.ro/rrch/

Rev. Roum. Chim.,
2016, *61*(6-7), 485-493

Dedicated to Professor Dumitru Oancea on the occasion on his 75th anniversary

STRUCTURAL AND MORPHOLOGICAL INVESTIGATIONS OF ZnO NANOSTRUCTURES OBTAINED BY HYDROTHERMAL METHODS AT DIFFERENT REACTION TIMES

Susana MIHAIU, Oana Cătălina MOCIOIU,* Alexandra TOADER, Irina ATKINSON, Jeanina PANDELE CUŞU, Cornel MUNTEANU and Maria ZAHARESCU

"Ilie Murgulescu" Institute of Physical Chemistry of Roumanian Academy, 202 Splaiul Independentei, Bucharest 060021, Roumania

Received November 3, 2015

ZnO nanostructure of rods and tubes was synthesized by hydrothermal method, using aqueous solutions of zinc-nitrate and hexamethylenetetramine. The experiments were conducted at 90°C for 2h, 4h, 8h and 24h. The influence of reaction time on the formation of ZnO based samples with different morphologies is investigated. The structural and morphological properties were examined by X-ray diffraction (XRD) and scanning electron microscopy (SEM) analyses. The XRD results confirmed the wurtzite crystal structure of ZnO in the synthesis and formation of a secondary phase after 8h of hydrothermal treatment. The SEM investigation shows the obtaining of nanorods after 2h of reaction and formation of nanotubes at prolonged reaction time. FT-IR studies were carried out in order to ascertain the presence of various functional groups in the obtained materials. DSC analysis confirmed the modifications observed in samples obtained at different reaction times.

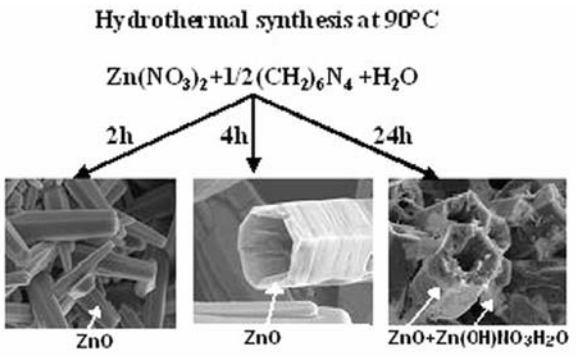

INTRODUCTION

Zinc oxide (ZnO) has a wide band gap (3.37eV) and large exciton-binding energy (60 meV) having a lot of applications such as photocatalyst,[1,2] dye sensitive solar cells,[3,4] UV-laser emission,[5] gas sensor,[6,7] piezoelectric devices,[4] optoelectronic devices,[5,8] transparent electronics,[9] antibacterial material.[10] Nanostructures with different morphologies show great potential for next-generation devices in optoelectronics,[11-16] biology,[10,16] solar cells[3,4] and sensors.[6,7]

ZnO has been obtained using several methods as sol–gel process,[1,12] wet chemical synthesis,[4,11] precipitation[9, 10,15] and hydrothermal synthesis.[3, 5-9, 13 -23] Some of the advantages of hydrothermal method are low temperature, simple devices and possibility to make green reactions. The sizes and shapes of ZnO nanostructures are very important in achieving the wished chemical, physical and electrical properties. The morphology of ZnO nanostructures is strongly influenced by preparation conditions.

* Corresponding author: omocioiu@icf.ro

Demoisson[19] demonstrated the effect of the metal salt concentration – [$Zn(NO_3)_2$] – in alkali medium (KOH) on the ZnO crystals growth in a supercritical domain. Many researchers[12-16,18] have used KOH or NaOH in hydrothermal synthesis to obtain ZnO rods. Lu[22] studied the influence of the alkaline sources used for hydrothermal synthesis on the morphology of the obtained ZnO particles. When NH4OH was used as alkaline source, ZnO crystallized in a rod-like morphology highly orientated on a-axis.[22] When the alkaline source used was methylethylenamine (MEA), diethylenamine (DEA) or triethylenamine (TEA), the ZnO powders crystallized as prismatic hexagonal flower-like or sphere-like morphology.[22] Jiang[23] obtained ZnO microspheres in a hydrothermal synthesis starting with zinc nitrate and anhydrous ethylenediamine. Organic additives such as polyethyleneglycol (PEG),[18] polyacrylic acid (PAA),[15] cetyl trimethyl ammonium bromide (CTAB),[16] ethylene diamine tetraacetic acid (EDTA),[21] were also used in the reaction to change the morphology of ZnO crystals in order to obtain better properties.

The zinc precursors used usually in the synthesis of nanomaterials are zinc acetate, zinc oxide, zinc nitrate and zinc chloride. The literature data of hydrothermal synthesis starting from zinc nitrate are presented in Table 1. It could be noticed that in all cases the ratio between Zn-precursor and HMTA is 1:1. The obtained morphologies for ZnO powders were evidenced.

The aim of work is the obtaining of ZnO starting from zinc nitrate tetrahydrated and hexamethylenetetramine (HMTA) in a molar ratio of 2:1, by hydrothermal synthesis at different reaction times. It has to be mentioned that this ratio between zinc nitrate and HMTA used for obtaining of ZnO nanorods/tubes was not reported before and it was approached from the scientific point of view in order to diminish the quantity of formaldehyde, formed during the synthesis process, which is a toxic compound.

Table 1

Hydrothermal synthesis for obtaining the nanopowders starting from zinc nitrate (selected references)

Raw materials	Hydrothermal synthesis	ZnO morphology	References
$Zn(NO_3)_2$ / $(CH_2)_6N_4$ /H_2O ratio 1:1 HCl (pH=1); KOH (pH=12)	200°C for 6h 450°C for 3h	nanorods (pH=7), flakes (pH=1) and flowers (pH=12)	Rayerfrancis[14]
$Zn(NO_3)_2{\cdot}6H_2O$/ $(CH_2)_6N_4$ /H_2O molar ratio 1:1	sonochemical at 70-50ºC	rods	Palumbo[20]
$Zn(NO_3)_2{\cdot}6H_2O$/ $(CH_2)_6N_4$/ NaOH/H_2O molar ratio 1:1:10	95ºC for 10 h/20 h 200ºC for 5 h	nanorod-based sphere-like superstructures	Gao[13]
$Zn(NO_3)_2{\cdot}6H_2O$/ NaOH/ PAA/ H_2O a, b) pH 5.6; c) pH 11.2 d) pH 12.5	90°C, 30 min	a-c) spherical nano-particles d) nanorods flower-like shape	Aimable[15]
$Zn(NO_3)_2$ $6H_2O$/ H_2O/ EtOH/ NaOH	60- 260 °C/16 h	60°C nanoparticles; 180- 220°C nanorods; 260°C flower	Reddy[17]
$Zn(NO_3)_2$ $6H_2O$ /$C_6H_8O_7$/ NaOH/ H_2O molar ratio 1:2.2:1; pH=14	120ºC, 17h	3D flower-like	Zhao[12]
$Zn(NO_3)_2 6H_2O$/ PEG/ H_2O/NH_4OH	120°C for 24h 450°C for 2h	dumbbell-shaped and flower-like	Jiang[18]
$Zn(NO_3)_2$ $6H_2O$/ NaOH/ CTAB/ H_2O molar ratio 1:2:1; pH~8	180°C for 3 h	nanorods	Moulahi[16]
$Zn(NO_3)_2$/ KOH/ H_2O molar ratio 1:4; pH=12.5-13	Supercritical conditions T = 411ºC P = 305 bar	rods	Demoisson[19]

EXPERIMENTAL

1. Materials and synthesis method

ZnO nanopowders were synthesized by the hydrothermal method using aqueous solutions of zinc nitrate tetrahydrate $Zn(NO_3)_2{\bullet}4H_2O$ (Merck) and hexamethylenetetramine (HMTA), $(CH_2)_6N_4$ (Merck). Precursor solution with concentration of 0.05 M was prepared using deionized water as solvent and a molar ratio of $Zn(NO_3)_2$ $4H_2O$: HMTA of 2:1. The solutions were mixed and stirred for 15 min at room temperature to obtain a clear solution. This precursor solution was used for hydrothermal synthesis of ZnO powders into Teflon lined stainless steel autoclaves. The autoclaves were heated in a conventional laboratory oven at a constant temperature of 90°C for 2h, 4h, 8h and 24h. After the reaction, the as-prepared powders were filtered and washed several times with hot deionized water at 85°C to remove residual salts and organic materials and then dried in air at room temperature.

2. Characterization

The XRD patterns were collected in 2Θ range between 10 to 80 with a speed of 5º min^{-1} and a step size of 0.02º. PDXL software from Rigaku, connected to ICDD data base was used for phase identification and lattice parameters calculation. The lattice parameters were refined by whole-powder pattern fitting method (WPPF) using the split pseudo-Voigt profile function and B-spline background model. The fitting quality of the experimental data was checked by using the following parameters: the goodness of fit S that should be close to1for a good fit and Rwp (weighted differences between measured

and calculated values) that should be close to or less than 10%. The crystallite size has been estimated using Scherrer Eq. for (001), (002) and (101) crystal planes using formula:

$$D = k \cdot \lambda / \beta \cdot \cos(\theta) \quad (1)$$

Where: k is a shape factor (taken as 0.94), β is the full width at half maximum of the intensity in radians, λ is the wavelength of the Cu Kα radiation (1.54056 Å) and θ is the Bragg's diffraction angle.

Vibration spectroscopic analysis was carried out using FT-IR Nicolet 6700 in 400-4000 cm^{-1} domain. The spectra of powders were recorded on the pellets of KBr.

The powder behavior at heating was determined by differential scanning calorimetry (DSC) with DSC Mettler Toledo 823e apparatus.

Morphologies of powders were evidenced with a scanning electron microscopy (SEM) using a high-resolution microscope FEI Quanta 3D model at an accelerating voltage of 20kV.

RESULTS

1. Scanning Electronic Microscopy

Fig. 1a-d show the morphologies of the ZnO nanorods and nanotubes obtained using the method presented above. It can be observed that at 2h of hydrothermal synthesis the nanorod structures growth and in cases of hydrothermal synthesis of 4h, 8h and 24h nanotubes were obtained. In Fig. 1d the nanotubes begin to be destroyed.

The cross section of the resulted nanorods shown in Fig. 1a is presented in Fig. 2. It can be noticed that the cross section presents a hexagonal form. The interesting aspect that should be mentioned is the darker color of the internal part. No direct experimental evidences are mentioned in the literature for the darker color of the internal part of the nanorods. We assume that it is a difference in the morphology of the internal and external part of the nanorods that facilitated the occurrence of the "Kirkendall effect".

2. X-Ray diffraction

Fig. 3 presents the XRD patterns of powders obtained after different reaction times. All powders showed a good crystallinity after hydrothermal

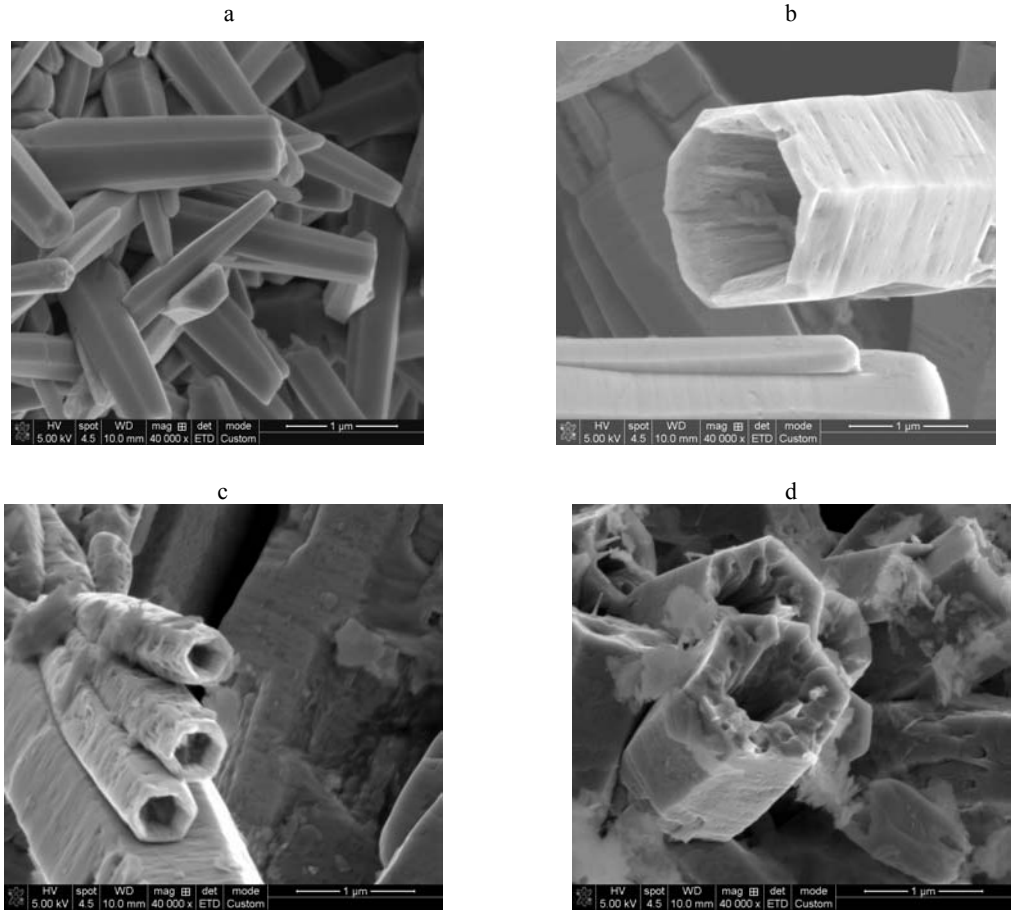

Fig. 1 – SEM of powders obtained by hydrothermal method at different reaction times:
a) 2h; b) 4h; c) 8h; d) 24h.

synthesis as can be observed from diffraction lines intensities. The XRD patterns of the powders obtained after 2 h and 4 h time of reaction show the diffraction lines corresponding to hexagonal ZnO phase (wurtzite structure) according to JCPDS file No.01-080-0075. In the case of powders obtained after 8h and 24h time of reaction, besides the diffraction lines from ZnO wurtzite structure additional diffraction lines corresponding to $Zn(OH)NO_3H_2O$ phase (JCPDS cards No. 01-084-1907) have been observed. The amount of the secondary phase increases with increasing the duration, time of the hydrothermal synthesis. The wurtzite phase decreases accordingly. The lattice parameters and crystallite size calculated from X-ray data are listed in Table 2. One can observe an increase of c/a ratio in comparison with the c/a ratio of the indexed value in JCPDS file. In a real ZnO crystal, the wurtzite structure deviates from the ideal arrangement, by changing the c/a ratio. In addition to composition, the lattice parameter can be affected by free charge, impurities, stress, and temperature. [24] In our case the presence of the secondary phase could contribute to the c/a ratio modification. The crystallite size was found to be in the range of 221-253 Å depending on the reaction times.

3. Infrared spectroscopy

By FTIR spectroscopy supplementary information on the structure of the resulted powders were obtained. The method allows evaluating the presence of the chemical groups from the vibration modes of their bonds. In Fig. 4 the infrared spectra of ZnO, which were acquired in the range of 400–4000 cm^{-1}, are shown. The stretching and the bending vibration of water are seen at 3359 cm^{-1} and 1636 cm^{-1}.[25-29] The bands at 1395, 1507 and 832 cm^{-1} are characteristic to vibration mode of NO_3^+ group.[29] The nitrate bands positions are shifted from those observed in the literature. This reflects the change in the structural environment of nitrate. In the spectra of powders at 8 and 24 hours of reaction (Fig. 1c and 1d) higher intensities of these bands are obtained probably due to the formation of secondary phase. The analysis of the spectra shows the existence of bands relating to the different vibration modes zinc–oxygen between 400 and 700 cm^{-1}. In fact, the bands situated at 506 and 421 cm^{-1} are attributed to the vibrations of elongation and of deformation respectively of the vibratory Zn–O.[25-29]

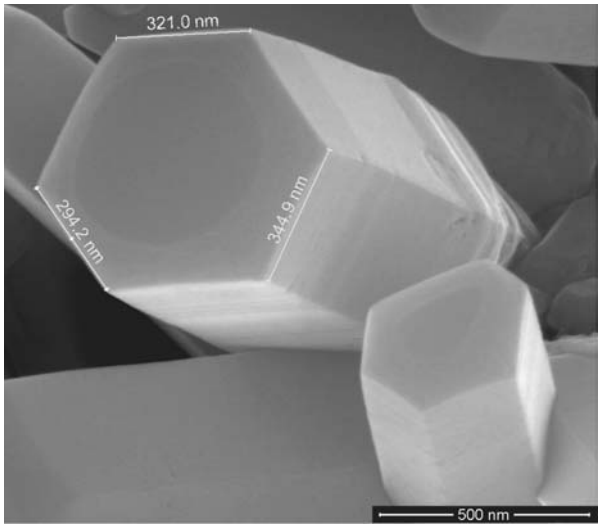

Fig. 2 – SEM image of cross section of nanorods obtained by hydrothermal method for 2h.

Table 2

The lattice parameters (a=b, c) and the average crystallite size (D_c)

Sample	Phase	Lattice parameters		c/a ratio	Dc (Å)	R_{wp}	S
		a=b (Å)	c(Å)				
ZnO 01-080-0075	ZnO	3.2539	5.2098	1.6011	-	-	-
ZnO-2h	ZnO	3.2526	5.2120	1.6024	241	7.93	1.1857
ZnO-4h	ZnO	3.2515	5.2113	1.6027	246	8.56	1.1946
ZnO-8h	ZnO	3.2519	5.2088	1.6018	253	8.51	1.2311
ZnO-24h	ZnO	3.2525	5.2127	1.6026	221	11.37	1.7979

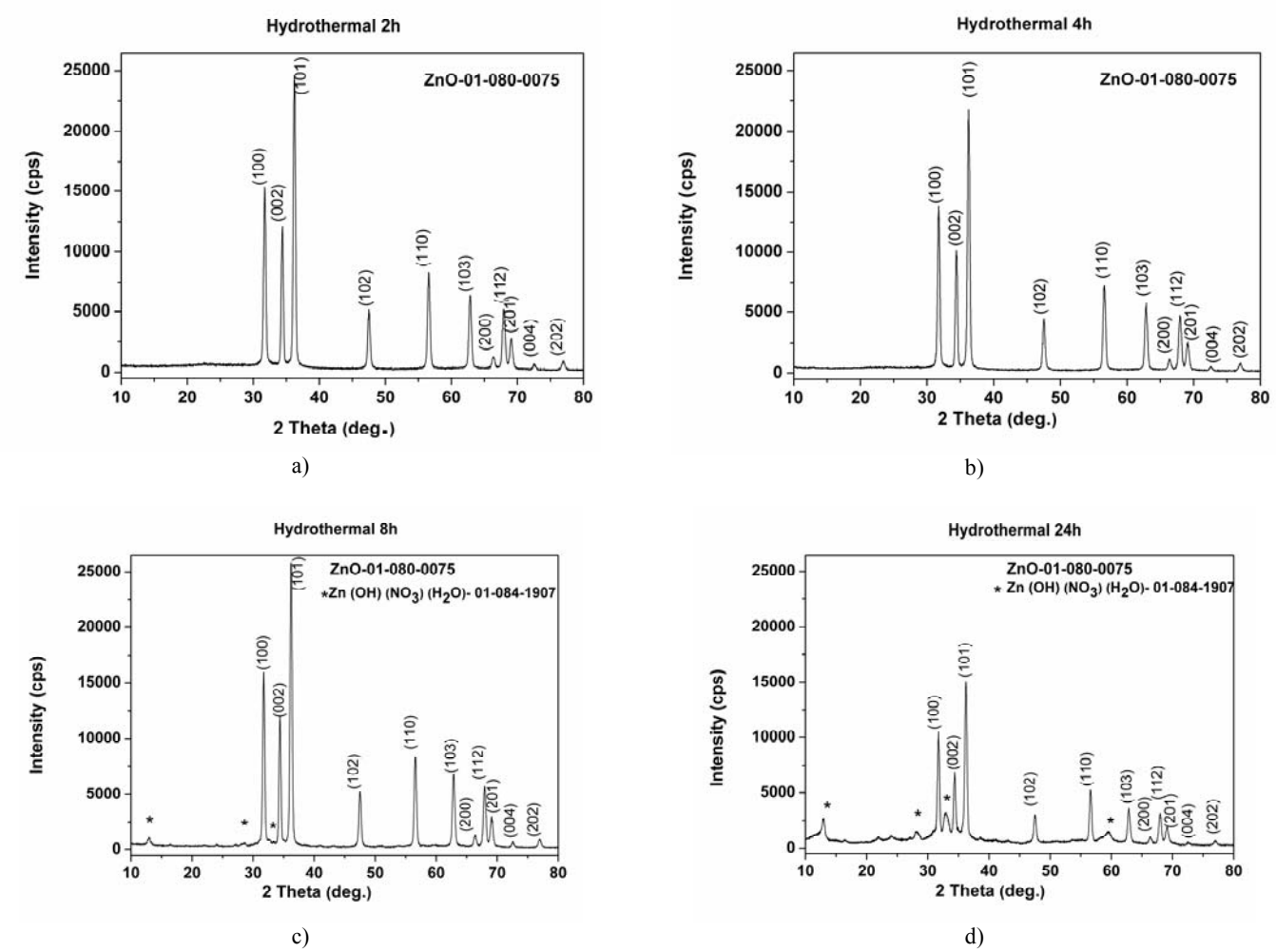

Fig. 3 – XRD patterns of powders obtained by hydrothermal method at different reaction times: a) 2h; b) 4h; c) 8h; d) 24h.

4. Differential scanning calorimetry

In Figs. 5a-5d the DSC analysis is presented. In the case of powders obtained by hydrothermal synthesis for 2h and 4h no thermal transformation can be seen in the thermograms. In Figs. 4c and 4d where the DSC curves for the powders obtained after 8h and 24h of reaction are given, endothermic effects can be observed at 237ºC and 264ºC, respectively. The effect can be assigned to decomposition of secondary phase with nitrate and hydroxyl evolution. The same observations were reported in case of study of the $Zn(OH)NO_3H_2O$ decomposition by DTA/TG.[27]

5. Mechanism of rods and tubes formation

The behavior of hexamethylenetetramine in the formation of ZnO can be given by the reactions presented below.[30] The decomposition of the hexamethylenetetramine in water, at 60°C, led to formation of ammonia and formaldehyde as can be seen in following reactions:

$$(CH_2)_6N_4 + 6H_2O \rightarrow 4NH_3 + 6HCHO \quad (1)$$

$$NH_3 + H_2O \rightarrow NH^+_4 + OH^- \quad (2)$$

The overall reactions in the solution are shown below: [31, 32]

$$Zn(NO_3)_2\,4H_2O + 2OH^- \rightarrow Zn(OH)_2 + + 2NO_3^- + 4H_2O \quad (3)$$

$$Zn(OH)_2 \rightarrow Zn^{2+} + 2OH^- \quad (4)$$

$$Zn^{2+} + 2OH^- \rightarrow ZnO + H_2O \quad (5)$$

In this work, after 2 h of reaction in hydrothermal conditions with high pressure and temperature of 90ºC the ZnO nanorods were obtained. The literature data show that the growth of ZnO crystals began with nucleation of hexagonal pellets followed by the addition of the

formed structural units on the (100) direction resulting the formation of nanorods.[30-34] In the case of studied samples the orientation on (100) direction is demonstrated by formation of nanorods, only. If the growing follows other directions then obtaining of nanorod is impossible and nanoflowers have been obtained as can be seen in references.[16-18] The ZnO nanotubes can be formed with one-step synthesis in suitable preparation conditions, as follows: (a) formation of crystal nucleus of ZnO at initial stage under hydrothermal reaction conditions; (b) additions of the structural units on the (100) direction to form of ZnO rods; (c) etching of the ZnO rods in solution, (d) Crater generation at the top of ZnO rods in solution; (e) Formation of the ZnO nanotubes in aqueous solution.

In the cases of our synthesis the nanorods and their growth according to the proposed mechanism – steps (a) and (b) – is presented in Fig. 6.

When reaction time is increased the formation of nanotubes takes place by craterlet generation on the top of ZnO nanorods, by disolving ZnO in reaction medium with formation of $Zn(OH)NO_3H_2O$. The initial stage of the transformation of nanorods into nanotubes is presented in Fig. 7.

It is reported that well defined side facets are highly stable as compared to the central portion of the hexagonal structure and are more defects prone.[35] Hence, slightly higher pH and heating temperature might enhance the etching in the central zone of the hexagonal disks, and create hollow structure.[35] This observation is confirmed by FTIR results (Fig. 4) that show even after washing of samples with hot water for removal of residues from the surface of nanotubes and nanorods; the FTIR spectra of samples at 2h and 4h identify weak bands of NO_3^- group, probably bonded on the core of nanorods.

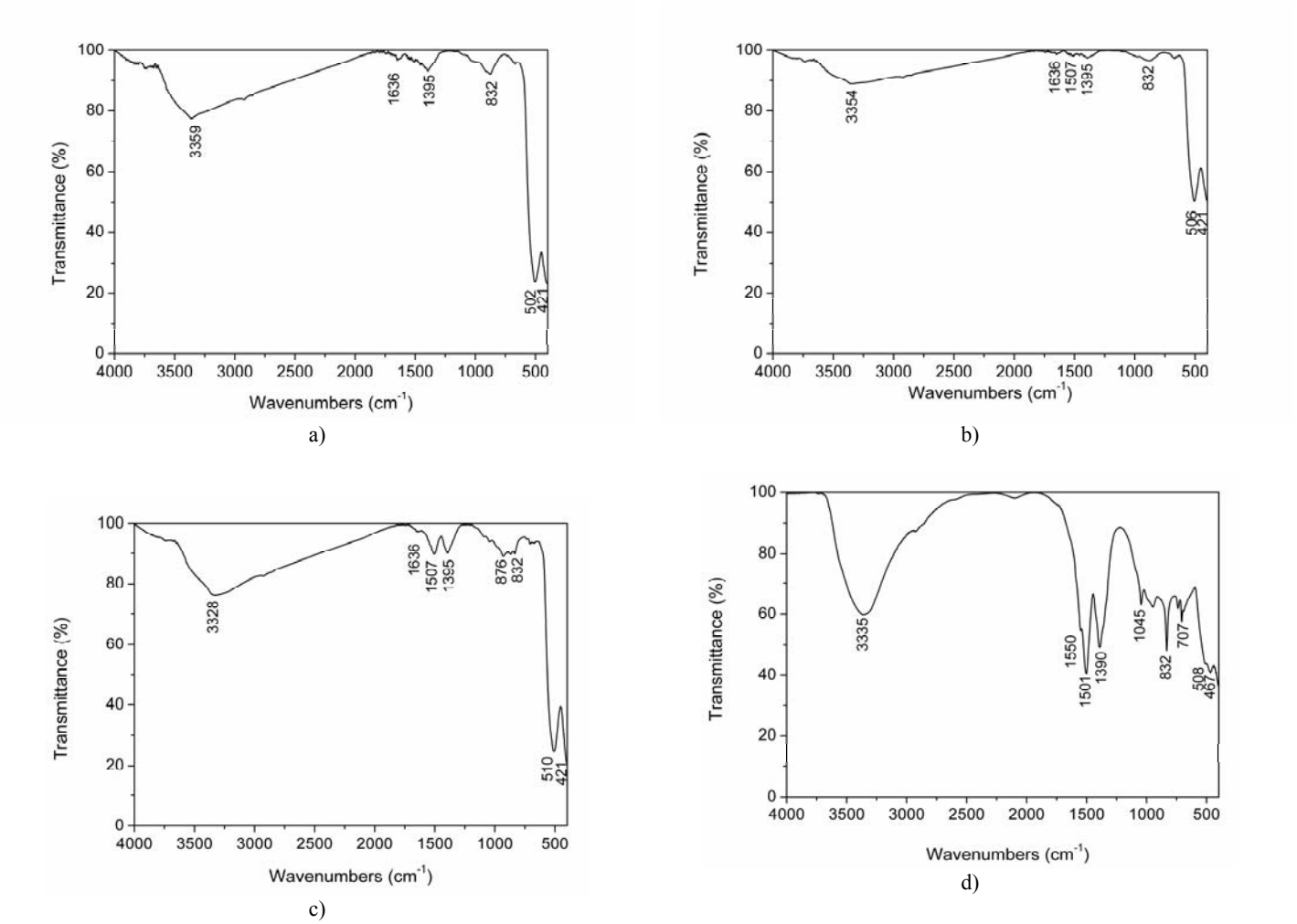

Fig. 4 – FT-IR spectra of powders obtained by hydrothermal method at different reaction times:
a) 2h; b) 4h; c) 8h; d) 24h.

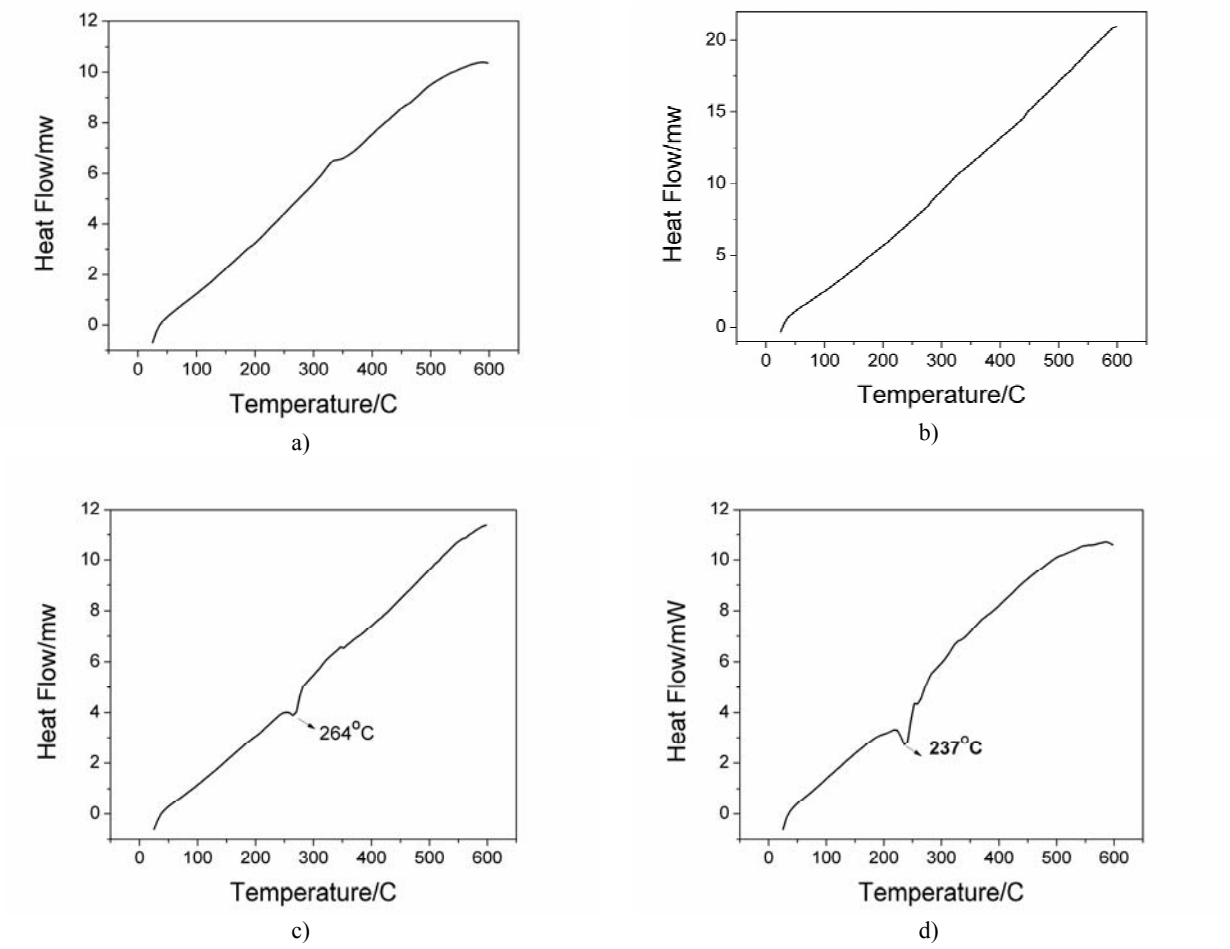

Fig. 5 – DSC of powders obtained by hydrothermal method at different reaction times:
a) 2h; b) 4h; c) 8h; d) 24h.

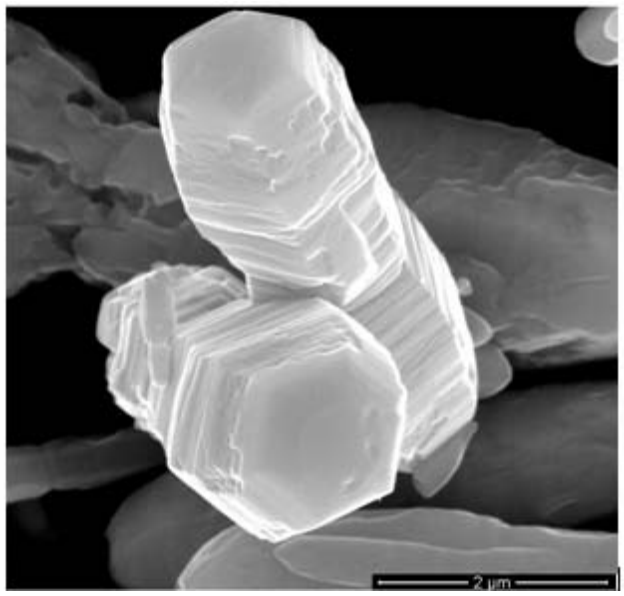

Fig. 6 – SEM image of nanorods and their growth according to the proposed mechanism.

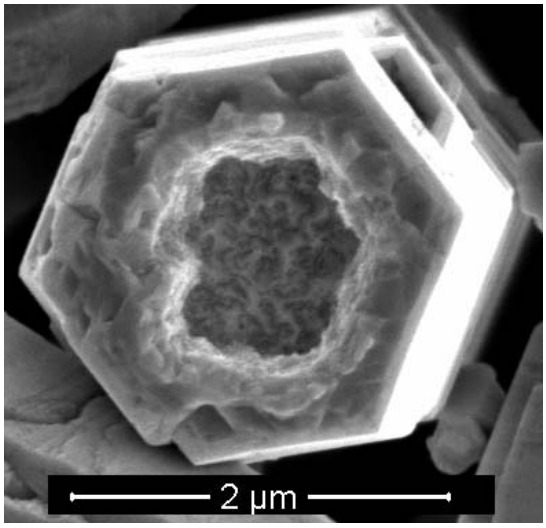

Fig. 7 – SEM image that presents the initial stage nanorods into nanotubes transformation.

According to literature data[36-38] the Kirkendall effect induces the void formation based on the different diffusion rates between two species. With increasing of reaction time, the inner core continuously reacts with OH^-, thus resulting in hollow tubular structures.[38] It must be noted that the consumed hydroxyl anions in reaction (3) are regenerated in reaction (4). Due to the fact that in the solution, NO_3^- ions also exist [see reaction (3)], the possible reaction of secondary phase formation takes place:

$$Zn^{2+} + NO_3^- + OH^- \rightarrow Zn(OH)NO_3H_2O \quad (6)$$

By increasing the reaction time over 8h, due to the interaction of ZnO with the reagents in solutions, hydrozincite is formed, identified as secondary phase by XRD and FTIR. The proposed mechanism is similar to that previously published for ZnO nanotubes based thin films.[33, 34, 39]

CONCLUSIONS

In summary, we have obtained hexagonal ZnO nanorods and nanotubes with high crystalline quality by hydrothermal method, starting from zinc nitrate tetrahydrate and hexamethylenetetramine. Even if the quantity of HMTA was decreased at half comparing with other synthesis from literature ZnO powders with different structure and morphologies were obtained, according to the SEM, FTIR XRD and DSC results that were in good agreement.

This work made obvious the effect of reaction time on the morphology of ZnO nanopowders. The ZnO nanorods were obtained after a hydrothermal process of 2h. In case of increasing the synthesis time to 4h nanotubes of ZnO were obtained. The ZnO powders with different morphologies obtained after 2h and 4h show wurtzite single phase. The powders obtained after 8h and 24h in hydrothermal conditions have nanotubes morphology and the secondary phase appears in their XRD patterns.

Acknowledgement. The financial support of apparatus acquisitions of EU (ERDF) INFRANANOCHEM – 19/01.03.2009 project is gratefully acknowledged.

REFERENCES

1. S. Saito, M. Miyayama, K. Koumoto and H. Yanagida, *J. Am. Ceram. Soc.,* **1985***, 68*, 40-43.
2. T.B. Ivetić, M.R. Dimitrievska, N.L. Finčur, Lj. R. Dačanin, I.O. Gútha, B.F. Abramović and S.R. Lukić-Petrović, *Ceram. Int.,* **2014**, 40*,* 1545-1552.
3. Y. Zhou, D. Li, X. Zhang, J. Chen and S. Zhang, *Appl. Surf. Sci.* **2012,** *261,* 759–763.
4. N. Karst, G. Rey, B. Doisneau, H. Roussel, R. Deshayes, V. Consonni, C. Ternon and D. Bellet, *Mater. Sci. Eng. B,* **2011,** *176,* 653-659.
5. M. Makkar, H. S. Bhatti and K. Singh, *J. Mater. Sci.: Mater. El.,* **2014,** *25,* 4822–4829.
6. Q. Zhou, W. Chen, L. Xu and S. Peng, *Sensors,* **2013,** *13,* 6171-6182.
7. W. Wang, Y.Tian, X.Wang, H. He, Y. Xu, C. He and X. Li, *J. Mater. Sci.,* **2013,** *48,* 3232-3238.
8. S.D. Senol, O. Ozturk and C. Terzioğlu, *Ceram. Int.,* **2015,** *41,* 11194–11201.
9. N. Kiomarsipour and R.S. Razavi, *Superlattice Microst.* **, 2012***, 52*, 704-710.
10. R. Wahab, A. Mishra, S.I. Yu, I.H. Hwang, J. Mussarat, A.A. Al-Khedhairy, Y.S. Kim and H.S. Shin, *Biomass Bioenerg.,* **2012**, *39,* 227-236.
11. H. Wang, C. Li, H. Zhao, R. Li and J. Liu, *Powder Technol.,* **2013***, 239*, 266-271.

12. X. Zhao, F.Lou, M. Li, X. Lou, Z. Li and J. Zhou, *J. Ceram. Int.*, **2014***, 40*, 5507-5514.
13. Y.J. Gao, W.C. Zhang, X.L. Wu, Y. Xia, G.S. Huang, L.L. Xu, J.C. Shen, G.G. Siu and P.K. Chu, *Appl. Surf. Sci.,* **2008**, *255,* 1982-1987.
14. A. Rayerfrancis, P.B. Bhargav, N. Ahmed, B. Chandra and S. Dhara, *Phys. B,* **2015,** *457,* 96-102.
15. A. Aimable, M. T. Buscaglia, V. Buscaglia and P. Bowen, *J. Eur. Ceram. Soc.,* **2010,** *30*, 591-598.
16. A. Moulahi, F. Sediri and N. Gharbi, *Mater. Res. Bull.,* **2012,** *47*, 667–671.
17. A.J. Reddy, R. H. Krishna, B.M. Nagabhushana, M.K. Kokila, H. Nagabhushana, C. Shivakumara and R.P.S. Chakradhar, *Spectrochim. Acta A,* **2015,** *139*, 262-270.
18. X. H. Jiang, S.Y. Ma, W.Q. Li, T.T. Wang, W.X. Jin, J. Luo, L. Cheng, Y.Z. Mao and M. Zhang, *Mater. Lett.,* **2015,** *142*, 299–303.
19. F. Demoisson, R. Piolet and F.Bernard, *J. Supercrit. Fluid,* **2015,** *97,* 268–274.
20. M. Palumbo, S. J. Henley, T. Lutz, V. Stolojan and S. R. P. Silva, *J. Appl. Phys,* **2008,** *104,* 074906.
21. W.L. Suchanek, *J. Cryst. Growth,* **2009***, 312,* 100-108.
22. C.-H. Lu, Y. C. Lai and R. B. Kale, *J. Alloy Compd.,* **2009,** *477,* 523–528.
23. H. Jiang, J. Hu, F. Gu and C. Li, *Particuology,* **2009,** *7,* 225–228.
24. M., Leszczynski, T. Suski, P. Perlin, H. Teisseyre, I. Grzegory, M. Bockowski, J. Jun, S. Porowski, K. Pakula, J.M. Baranowski, C.T. Foxon and T.S. Cheng, *Appl. Phys. Lett.*, **1996***, 69*, 73-77.
25. M. Zaharescu and O. C. Mocioiu, "Infrared Spectroscopy" in book "Chemical Solution Deposition of Functional Oxide Thin Films", T. Schneller, R. Waser, M. Kosec and D. Payne, Springer-Verlag Wien, 2013, Chapter 9, p. 213-230.
26. S. Mihaiu, M. Gartner, M. Voicescu, O. C. Mocioiu and M. Zaharescu, *Opt. Adv. Mater.-R.C.,* **2009,** *3*, 884-890.
27. S. M. Mihaiu, J. Madarasz, G. Pokol, I. M. Szilagyi, T. Kaszas, O. C. Mocioiu, I. Atkinson, A. Toader, C. Munteanu, V. E. Marinescu and M. Zaharescu, *Rev. Roum. Chim.,* **2013***, 58*, 335-345.
28. C. Pholnak, C. Sirisathitkul and D. J. Harding, *J. Phys. Chem. Solids,* **2011,** *72*, 817–823.
29. T. Biswick, W. Jones, A. Pacu, E. Serwicka and J. Podobinski, *J. Solid State Chem,* **2007,** *180,* 1171–1179.
30. S.D.G. Ram, G. Ravi, A. Athimoolam, T. Mahalingam and M. Anbu Kulandainathan, *Appl. Phys. A,* **2011,** *105*, 881–890.
31. N. Kiomarsipour and R. S. Razavi, *Ceram. Int.,* **2013**, *39,* 813-818.
32. N. Kiomarsipour and R. S. Razavi, *Ceram. Int.,* **2014**, *40,* 11261-11268.
33. F. Sun, X. Qiao, F. Tan, W. Wang and X. Qiu, *Appl. Surf. Sci.* **2012**, *263*, 704–711.
34. H. Gao, G. Fang, M. Wang, N. Liu, L. Yuan, C. Li, L. Ai, J. Zhang, C. Zhou, S. Wu and X. Zhao, *Mater. Res. Bull.,* **2008**, *43, 3*345-3351.
35. S. Ameen, M.S. Akhtar, Y.S. Kim, O-B. Yang and H.-S. Shi, *Electrochim. Acta,* **2011**, *56,* 1111-1116.
36. Y. Yin, R.M. Rioux, C.K. Erdonmez, S. Hughes, G.A. Somorjai and A.P. Alivisatos, *Science,* **2004**, *304*, 711-714.
37. B Liu and D. Xue, *Adv. Mater.,* **2008**, *20,* 2622-2626.
38. J. Guo, X. Zhang, T. Zhang, T. Zhou, X. Zhang and Z. Quan, *Mater. Lett.,* **2015**, *141*, 288-290.
39. X. Ma, M. Gao, J. Zheng, H. Xu and G. Li, *Physica E,* **2010,** *42,* 2237–2241.